Journal of Power Sources 196 (2011) 5272–5276

Contents lists available at ScienceDirect

Journal of Power Sources

journal homepage: www.elsevier.com/locate/jpowsour

Short communication

Imaging of membrane electrode assemblies of proton exchange membrane fuel cells by X-ray computed tomography

Andreas Pfrang[a,*], Damien Veyret[a], Gaby J.M. Janssen[b], Georgios Tsotridis[a]

[a] Institute for Energy, Cleaner Energy Unit, Joint Research Centre, European Commission, P.O. Box 2, 1755 ZG Petten, The Netherlands
[b] Department of Hydrogen and Clean Fossil Fuels, Energy Research Centre of the Netherlands ECN, P.O. Box 1, 1755 ZG Petten, The Netherlands

ARTICLE INFO

Article history:
Received 17 June 2010
Received in revised form 7 September 2010
Accepted 8 September 2010
Available online 16 September 2010

Keywords:
PEM fuel cell
Membrane electrode assembly
Gas diffusion layer
Computed tomography
Micro porous layer

ABSTRACT

X-ray computed tomography was applied for the 3D imaging of membrane electrode assemblies (MEAs) together with two attached gas diffusion layers. These samples were investigated as prepared and after voltage cycling. It was possible to achieve sub-μm resolution using a lab-based stand-alone tomography system as well as a tomography add-on for a scanning electron microscope. The carbon fibres of the gas diffusion layers could be clearly resolved and the catalyst layers could be visualized.

X-ray computed tomography data were also used for the validation of results from scanning electron microscopy of cross-sections of membrane electrode assemblies where the sample is exposed to significant mechanical loads during sample preparation. More specifically, it was shown that the cracks observed in catalyst layers by scanning electron microscopy already exist in the membrane electrode assembly as prepared and are not a result of sample preparation. Finally it was shown that the crack density in the catalyst layers does not significantly change during voltage cycling which suggests that crack formation is not a principal cause of the observed performance decay of the MEA.

© 2010 Elsevier B.V. All rights reserved.

1. Introduction

The membrane electrode assembly (MEA) together with the gas diffusion layers (GDLs) forms the core of a proton exchange membrane fuel cell (PEMFC). As the key reactions of a fuel cell take place inside the MEA, it is crucial to investigate its structure and possible aging effects. Scanning electron microscopy is one of the standard techniques not only for the characterization of GDLs, but also of the MEA or even of catalyst material [1–6]. Additionally – among many other more specialized techniques which are applied – transmission electron microscopy and X-ray diffraction should be mentioned as standard techniques [3–6] for the characterization of catalyst structure.

In recent years, improvements in resolution allow not only application of synchrotron radiation based 3D imaging techniques [7–9], but also the use of lab based X-ray computed tomography (CT) for the investigation of gas diffusion layers [10–12]. Both techniques require only minimal sample preparation and reach sub-μm resolution which is sufficient for the imaging of carbon fibres with typical diameters between 5 and 10 μm. CT has also been used for the investigation of wetting behaviour of gas diffusion layers [13,14] and the investigation of PEMFC membranes and membrane electrode assemblies [15].

In this paper, X-ray computed tomography is evaluated with respect to its applicability for the investigation of a membrane electrode assembly together with the two corresponding gas diffusion layers.

2. Materials and methods

2.1. Membrane electrode assemblies

Membrane electrode assemblies were prepared and investigated as prepared and after use, i.e. after fast voltage cycling.

The MEAs had an active surface of 7 cm^2 and consisted of the following components: Nafion® NRE212CS membrane from DuPont, Sigracet® GDL31BC (impregnated with polytetrafluoroethylene, PTFE and equipped with a micro porous layer, MPL) from SGL Carbon and Hispec®9100 catalyst from Alfa Aesar; the catalyst loading was 0.4 mg cm^{-2} for cathode and anode (57 wt% Pt on high surface area carbon black). The Nafion® to carbon weight ratio in the catalyst layer was 0.55. The preparation of the MEAs has been described elsewhere [16]. The used MEA was taken from a previous study into the degradation of MEAs under fast voltage cycling. During the fast voltage cycling, an MEA was operated with H_2 and air and underwent 30,000 square wave cycles between 0.7 V (IR-corrected) and 0.9 V (IR-corrected), or OCV when OCV dropped below 0.9 V, with 30 s hold at each potential. Further details on the investigation of the used MEA can be found in [17].

* Corresponding author. Tel.: +31 224 56 5047; fax: +31 224 56 5623.
E-mail address: andreas.pfrang@ec.europa.eu (A. Pfrang).

0378-7753/$ – see front matter © 2010 Elsevier B.V. All rights reserved.
doi:10.1016/j.jpowsour.2010.09.020

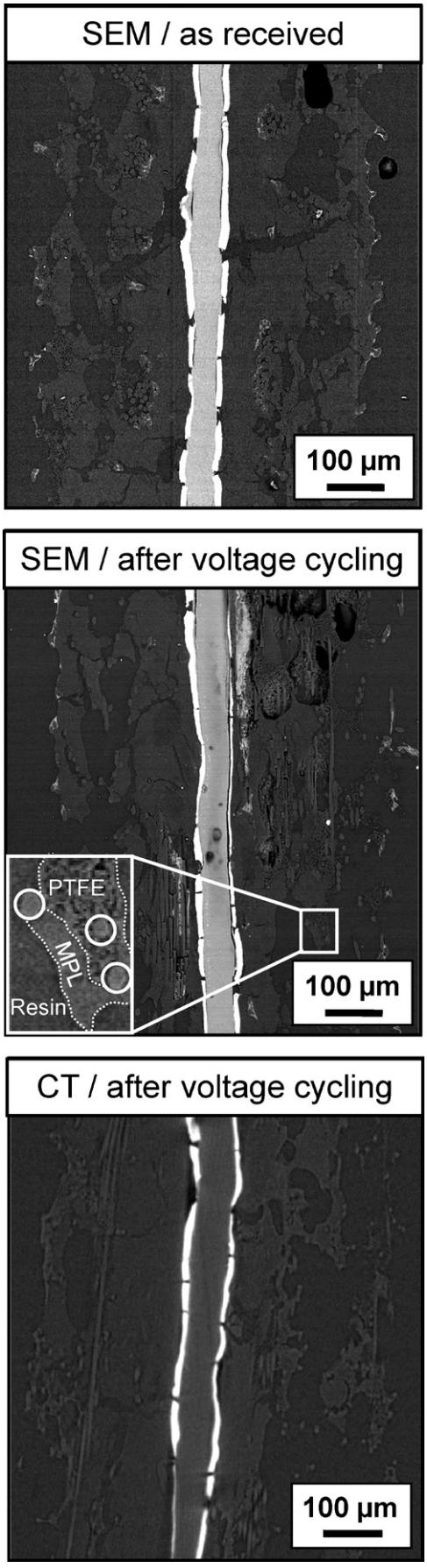

2.2. Scanning electron microscopy

Cross-sections were prepared by embedding an MEA in Epofix resin followed by grinding and polishing. A JEOL-JSM-6330F scanning electron microscope (SEM) was used to image cross-sections of the membrane electrode assemblies.

2.3. X-ray computed tomography

X-ray computed tomography was used to investigate the membrane electrode assemblies. Strips with widths between 1 and 3 mm and lengths up to 10 mm were cut from each membrane electrode assembly. These strips were investigated using different systems:

- A nanotom® CT system (GE Sensing & Inspection Technologies, phoenix X-ray, Wunstorf, Germany). This system includes a 180 kV X-ray tube and a 2D X-ray detector with 2300 × 2300 pixels.
- An X-ray Ultra Microscope (XuM, Gatan, Pleasanton, US) which is an add-on for a scanning electron system and uses the SEM electron beam to produce X-rays. The Gatan XuM was used mounted on a JEOL 6610LV SEM which was equipped with a tungsten filament as electron source and was operated at 30 kV.

The chosen voxel size for the two systems was 0.8 and 0.9 μm, respectively. Due to the different density of the different components, they exhibit different ranges of gray values in the CT dataset. For segmentation after reconstruction, a certain gray-value threshold was chosen to generate a 3D model from the gray-valued 3D dataset. Voxels darker than this threshold gray-value were assigned to air and voxels brighter than this threshold were assigned to solid material.

3. Results

Membrane and electrode layers appear bright and are clearly visible in the centre of the SEM micrographs of Fig. 1 (top and middle). While the thicknesses of anode and cathode electrode layer are very similar in the MEA as received, the thickness of the cathode electrode layer is significantly reduced after voltage cycling. In the GDLs, several holes at the surface of the cross-sections with diameters of a few 10 μm are visible in both SEM photos. Carbon fibres are visible already at this magnification, but the contrast is not very clear with respect to PTFE and MPL material. The fibres appear to be covered by a solid phase, consisting of PTFE and MPL material, over the whole thickness of the GDL. At higher magnification (see inset of Fig. 1), not only the fibres are clearly visible (marked by circles), but also PTFE and MPL material can be separated.

The bottom image of Fig. 1 shows a cross-section of the reconstructed CT data of the MEA after voltage cycling. No segmentation was performed for the visualization. As in SEM, the catalyst layers appear brighter than the surrounding material (and air). The carbon fibres are visible, and are partially covered by a solid phase.

Fig. 2 shows a reconstruction of the CT data of an MEA after voltage cycling after segmentation. On the left side of Fig. 2, the whole investigated volume is shown; the threshold for segmentation is different for the two parts separated by the clipping plane: left of the clipping plane, all components of the sample are visible while

Fig. 1. Cross-section of a membrane electrode assembly as prepared (scanning electron micrograph, top) and after voltage cycling (scanning electron micrograph, middle and reconstructed X-ray computed tomography data, bottom). The scanning electron micrographs were acquired at 15 kV; backscattered electrons were detected for imaging. In the magnified inset of the middle micrograph, the different components – PTFE, micro porous layer (MPL), carbon fibres (marked by circles) and resin (as embedding material) – are marked.

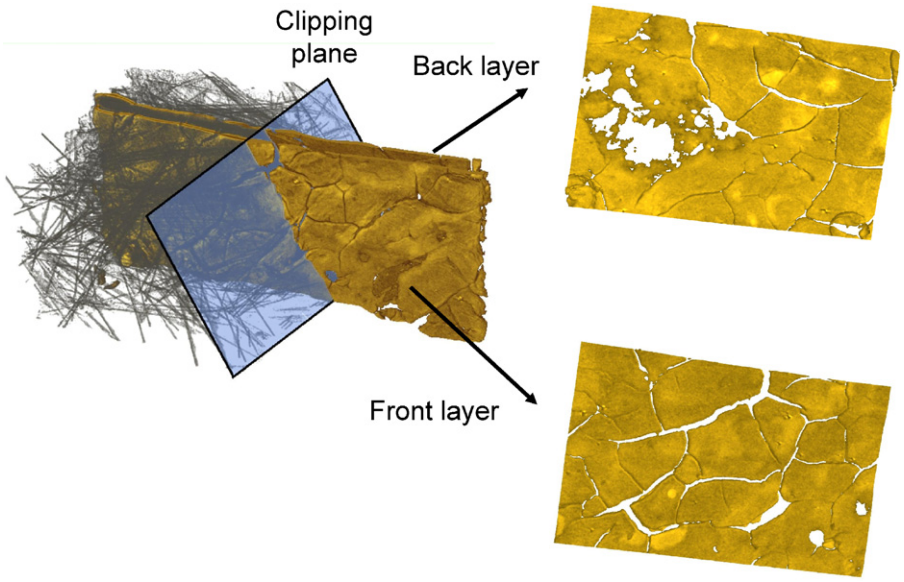

Fig. 2. Membrane electrode assembly of a used PEM fuel cell (thickness 700 μm) as imaged by X-ray computed tomography. On the right side of the image (marked by the clipping plane), the gray level threshold for segmentation is adjusted to show only the catalyst layers.

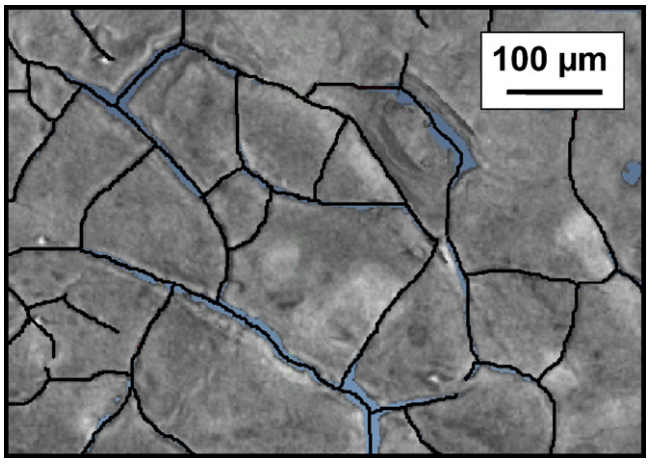

Fig. 3. Top view of a catalyst layer of a used PEM fuel cell as imaged by X-ray computed tomography. The cracks are marked by black lines.

on the right side of the clipping plane only the catalyst layers are shown. This was achieved by increasing the gray level threshold which means that only voxels with high X-ray absorption are visualized. Front and back catalyst layers are shown on the right side of Fig. 2. Cracks are visible in both – front and back – catalyst layers. In the back layer, irregularly shaped holes are visible as well.

Fig. 3 illustrates the determination of crack density based on CT 2D images of the catalyst layers (denoted as CT 2D). In a first step, the catalyst layer is visualized by choosing an appropriate gray level threshold for segmentation (see also Fig. 2). Then the cracks are marked manually (see Fig. 3) and crack density is calculated based on the overall length of the cracks and the examined volume which are both evaluated automatically based on the manual marks using standard image software. For comparison, the crack density is also determined on cross-sections based on reconstructed CT data by counting cracks (denoted CT 1D, compare e.g. Fig. 1, bottom).

The crack density was also determined based on SEM images by counting the cracks in SEM images of cross-sections (see. Fig. 1, top and middle) and dividing by the investigated length of the catalyst layer. The results of the determination of the crack density by SEM and CT are summarized in Table 1.

4. Discussion

The comparison of results from X-ray computed tomography with scanning electron microscopy allows an evaluation of CT's potential for the investigation of an MEA with two gas diffusion layers attached. At first sight, CT and SEM images of cross-sections as shown in Fig. 1 appear quite similar. While the maximum resolution for many CT systems is already reached with 0.8 μm in the bottom image of Fig. 1, much higher resolutions are possible in SEM. But on the other hand SEM is limited to the investigation of surfaces – which requires the preparation of a dedicated cross-sectional sample – while CT allows the imaging of cross-sections based on the 3D data of intact, non-embedded samples. This means that artefacts due to sample preparation can be avoided almost completely using X-ray computed tomography as it is a non-invasive technique.

Accordingly, no artefacts from preparation are visible in the CT cross-section (Fig. 1 bottom), while the inhomogeneities that are visible in SEM photos (Fig. 1, top and middle) at the surface of the cross-sections with diameters of a few 10 μm could stem from an incomplete penetration of the GDLs during the infiltration step of the sample preparation procedure.

While it is generally possible to image the PTFE quite clearly against carbon fibres using SEM [1], this has not been possible applying X-ray computed tomography as there is no sufficient difference in the mass densities – and consequently in the X-ray absorption – between carbon fibres and PTFE.

The investigated GDLs consist in addition to PTFE and carbon fibres also of a micro porous layer (MPL). In the SEM images, the whole GDL seems to be penetrated by solid material, i.e. PTFE and MPL material. Closer examination of the SEM images of Fig. 1 already allows an approximate discrimination of PTFE from MPL

Table 1
Crack densities of catalyst layers of membrane electrode assemblies as prepared and after voltage cycling as determined by X-ray computed tomography and scanning electron microscopy.

Sample	Crack density (mm^{-1})	
	SEM	CT 2D (CT 1D)
MEA as prepared	10	14 (11)
MEA after cycling	11	15 (9)

material as PTFE appears to exhibit a rougher surface (see inset in Fig. 1), but a dedicated SEM investigation would show this difference even clearer. Still, the question remains if this distribution of MPL material over the whole thickness of the GDL is present already in the GDL as received or due to sample changes during SEM sample preparation. By comparing with the CT cross-section – where no discrimination of PTFE from MPL material is possible – it can be concluded that the SEM photos represent sufficiently well the original structure of the GDLs even though the PTFE/MPL material appear more fractured in SEM than in CT. This in turn, could be result of the SEM sample preparation procedure.

In the SEM images of Fig. 1 cracks in the catalyst layer are visible. In our laboratory, such cracks are commonly observed in SEM images of catalyst layers screenprinted on Sigracet® GDL31BC, independent of the exact composition of the layer. It is difficult to judge only on basis of the SEM data if these cracks result from SEM sample preparation or if they exist already in the freshly prepared MEA. Furthermore, the SEM image of a MEA after voltage cycling shows that the thickness of the cathode catalyst layer is reduced at certain locations. Such a reduction of the layer thickness must first of all be ascribed to oxidation of the carbon black support of the electrocatalyst. This will lead to loss of functionality of the electrocatalyst. It should be noted that the voltage cycling resulted for this MEA in a significant loss of performance which was ascribed to irreversible changes in the combination of GDL/MPL/catalyst layer [17].

For the segmentation of CT data, the selection of proper thresholds to separate different materials is crucial. Even though the catalyst layer exhibits a certain porosity and Pt is mixed with carbon black and Nafion, the catalyst layer can be identified easily in the CT dataset because it exhibits the highest absorption capacity of the whole membrane electrode assembly. This is mainly due to the high density of Pt as compared to the other elements present in the MEA. Still the selection of the threshold for the catalyst layer is somewhat arbitrary, as it is composed out of different materials and the fractions of the different components will vary with location. The selection of a threshold for the carbon fibres could be based on comparison with SEM data [1]. The carbon fibre could be resolved by CT, additionally the distribution of further solid material – consisting of MPL material and PTFE – could be determined. As the gray value ranges of carbon fibres, MPL material and PTFE overlap, a discrimination using gray value thresholding is not possible, but the application of different, partly morphology based segmentation algorithms might allow this discrimination in the future.

The CT reconstruction of Fig. 2 of a MEA after voltage cycling shows the full 3D structure of the catalyst layers with a manually selected threshold that results in a catalyst layer thickness corresponding to SEM data. This structure allows confirming that the cracks do not result from SEM sample preparation and indeed already exist in the MEA as prepared (CT data not shown) and still exist after voltage cycling. On the back electrode of Fig. 2 – in addition to the cracks – irregularly shaped holes are observed which could result from a thinning of the electrode during voltage cycling.

The density of cracks in the catalyst layers as determined by SEM and CT (see Table 1) does not show a significant difference in crack densities before and after voltage cycling. Furthermore, there is also no significant difference in crack densities after voltage cycling between anode and cathode side. These observations show that the cracks are not a result of the cycling, and suggest that the cracks do not directly contribute to degradation of the catalyst layers. No preferred orientation of the cracks was found (compare Figs. 2 and 3) and while cracks in the catalyst layer have been observed earlier [18], in that case they were preferably aligned along a certain direction. It is still unclear, if the cracks actually should be avoided during MEA preparation or if they actually are relevant for the proper functioning of these MEAs, e.g. with regard to water management.

When comparing crack densities determined based on CT and SEM data, the crack densities determined by SEM and based on CT cross-sections agree reasonably while the CT crack densities determined on 2D images of the catalyst layer are higher. This may be caused by the different methods of determination: for CT 2D, lengths of cracks are measured and because of their better visibility as compared to looking for a crack in a cross-section (SEM or CT 1D), this may result in systematically higher crack densities.

It was possible to image the complete assembly of MEA and two GDLs on both CT systems, even though the Gatan XuM works at much lower X-ray energies, implying lower penetration depths. Due to the relatively light elements – except for the Pt catalyst which is only present in small amounts – also SEM mounted X-ray CT systems still are suitable for the investigation.

Generally – while SEM surely has several advantages like higher resolution or better PTFE identification capacity – CT only requires minimal sample preparation, i.e. artefacts can be avoided. Furthermore, CT offers statistical advantages as an investigation of a volume, typically a fraction of a mm^3, already allows averaging over multiple cross-sections. Finally, some features can only be properly identified in the 3D structure and the 3D structure model determined by CT can be directly used for calculating physical properties or for simulating fuel cell performance.

5. Conclusion

X-ray computed tomography – using stand-alone as well as SEM based systems – is a suitable technique for the 3D imaging of membrane electrode assemblies with attached gas diffusion layers. This method can reach sub-μm resolution on these samples and only requires minimal sample preparation.

CT is therefore also suitable for the validation of results obtained by SEM on cross-sections where the sample is exposed to significant mechanical loads during sample preparation. More specifically, it was shown that the cracks observed in catalyst layers by SEM already exist in the membrane electrode assembly as prepared and are not a result of SEM sample preparation.

X-ray computed tomography can be an important complementary investigation technique for membrane electrode assemblies – with or without attached gas diffusion layers. The 3D structure model determined by CT can be the starting point for more detailed investigations, e.g. for the calculation of physical properties or simulation of fuel cell performance.

Acknowledgements

This work has been carried out within the multi-year program of the European Commission's Joint Research Centre under the auspices of the FCPOINT action. The authors would like to thank Gatan (Pleasanton, US) and Jeol Europe (Croissy sur Seine, France) for CT measurements, Marijke Roos and Marcel Bregman (ECN) for SEM sample preparation and analysis, and Marc Steen for critical reading of the manuscript.

References

[1] M. Schulze, M.V. Bradke, R. Reissner, M. Lorenz, E. Gülzow, Fresen. J. Anal. Chem. 365 (1999) 123–132.
[2] M.F. Mathias, J. Roth, J. Fleming, W. Lehnert, Diffusion media materials and characterisation, in: W. Vielstich, H.A. Gasteiger, A. Lamm (Eds.), Handbook of Fuel Cells – Fundamentals, Technology and Applications, John Wiley, 2003, pp. 517–537.
[3] E. Guilminot, A. Corcella, F. Charlot, F. Maillard, M. Chatenet, J. Electrochem. Soc. 154 (2007) B96–B105.
[4] K.L. More, R. Borup, K.S. Reeves, ECS Trans. 3 (2006) 717–733.
[5] L. Jing, H. Ping, W. Keping, M. Davis, Y. Siyu, ECS Trans. 3 (2006) 743–751.

[6] P.J. Ferreira, G.J.O. La, Y. Shao-Horn, D. Morgan, R. Makharia, S. Kocha, H.A. Gasteiger, J. Electrochem. Soc. 152 (2005) A2256–A2271.
[7] J. Becker, R. Flückiger, M. Reum, F.N. Büchi, F. Marone, M. Stampanoni, J. Electrochem. Soc. 156 (2009) B1175–B1181.
[8] J. Becker, V. Schulz, A. Wiegmann, J. Fuel Cell Sci. Technol. 5 (2008), art. no. 021006.
[9] I. Manke, C. Hartnig, N. Kardjilov, H. Riesemeier, J. Goebbels, R. Kuhn, P. Krüger, J. Banhart, Fuel Cells 10 (2010) 26–34.
[10] H. Ostadi, K. Jiang, P.D. Prewett, Micro Nano Lett. 3 (2008) 106–109.
[11] H. Ostadi, P. Rama, Y. Liu, R. Chen, X.X. Zhang, K. Jiang, J. Membr. Sci. 351 (2010) 69–74.
[12] A. Pfrang, D. Veyret, F. Sieker, G. Tsotridis, Int. J. Hydrogen Energy 35 (2010) 3751–3757.
[13] P.K. Sinha, P. Halleck, C.Y. Wang, Electrochem. Solid-State Lett. 9 (2006) A344–A348.
[14] A. Bazylak, Int. J. Hydrogen Energy 34 (2009) 3845–3857.
[15] F.H. Garzon, S.H. Lau, J.R. Davey, R.L. Borup, ECS Trans. 11 (2007) 1139–1149.
[16] G.J.M. Janssen, E.F. Sitters, A. Pfrang, J. Power Sources 191 (2009) 501–509.
[17] F.A. De Bruijn, V.A.T. Dam, G.J.M. Janssen, R.C. Makkus, ECS Trans. 25 (2009) 1835–1847.
[18] F.E. Hizir, S.O. Ural, E.C. Kumbur, M.M. Mench, J. Power Sources 195 (2010) 3463–3471.